

Comparison of Numerical Methods for Solving the Convection-Diffusion Equation in 2D

Edgar Lobaton

Seattle University

Ubaldo Rodríguez Bernier

University of Puerto Rico-Cayey

Leah N. Shilling

Slippery Rock University

Abstract

A numerical analysis of the error generated by three deterministic particle methods approximating the solution to the convection-diffusion equation in two-dimensions is presented. This analysis determines the method that yields the greatest degree of accuracy. The method of analysis is broken into two sections: relative error analysis and a conservation analysis, with a focus on the study and comparison of a continuous and discontinuous case. Some examples of the solution of the convection-diffusion equation with a prescribed flow are modeled.

1 Introduction

In this paper, we study the convection-diffusion equation in two dimensions, which can be thought of physically as the diffusion of heat on a plate with respect to time and a prescribed flow. Equations describing this type of motion are often difficult to solve analytically, which is why the use of numerical methods (such as the particle methods addressed here) to approximate the solution has increased in recent years. The convergence of the three particle methods here employed, namely the particle strength exchange method (PSE) along with two of its variations, has been proven in [2], and their theoretical accuracy is known. However, the methods have not yet been used in practice, so the numerical degree of accuracy of these approximations remained unknown. Our research centers around the error analysis of these methods with the goal of understanding this unknown accuracy in the practical implementation of the methods while investigating the conservation properties of each method.

The error of these methods is primarily based upon the size of the discretized domain and the clustering of the particles. The number of particles analyzed, along with the grid spacing affecting inter-particle distance, are vital parameters in our research. While lack of previous error analysis leaves us without concrete results, we do possess some knowledge of results to come. It was found in [2] that the difference

between the numerical solution, denoted by Γ^h , and the solution of the convection-diffusion equation, denoted by Γ , satisfies the following discrete L^2 -norm error bound estimate:

$$\|\Gamma^h - \Gamma\|_{0,2,h} \leq C\nu \left(\sigma^d + \frac{h^m}{\sigma^{m+2}} + \frac{h^{m+3/2}}{\sigma^{m+5}} \right) \quad (1)$$

where h represents the previously mentioned inter-particle distance and ν is the diffusivity. C is a constant independent of ν and numerical parameters. It was asserted that the value of σ must be larger than h , yet small enough so that the terms in the error bound balance. The exponent of σ , d , is the order of the approximation of the Laplacian by the operator Q discussed later, while m is dependent upon the initial conditions and smoothness of the flow. Smaller regularization errors can be reached with high-order kernels that yield larger values of d . By manipulating the appropriate parameters, along with other factors discussed later, we ascertain the values that produce the least error while conserving the necessary properties. In doing so, we determine the method that provides the highest accuracy of approximation. Additionally, we use the approximation methods to model convection-diffusion problems. That is to say, we model the flow and diffusion of heat as time changes.

2 Background

We begin by defining the general convection-diffusion equation as:

$$\frac{\partial \Gamma}{\partial t} + (\mathbf{u} \cdot \nabla) \Gamma = \nu \Delta \Gamma, \quad \nabla \cdot \mathbf{u} = 0 \quad (2)$$

$$\Gamma(\mathbf{x}, 0) = \Gamma_0(\mathbf{x}), \quad \mathbf{x} \in \mathbb{R}^2, \quad (3)$$

where $\mathbf{u}(\mathbf{x}, t)$ is a prescribed flow and Γ may represent heat on an infinite plate. The study of the solution of this equation and the methods used for approximation require additional knowledge of various concepts. These concepts are briefly described in the following sections.

2.1 Blobs

Definition 1 Let $f(x) : \mathbb{R} \rightarrow \mathbb{R}$ be a smooth, even function. $f(x)$ is called a blob if $\int_{-\infty}^{\infty} f(x) dx = 1$.

A blob f_δ in one dimension is defined as a scaled version of a ,

$$f_\delta(s) = \frac{1}{\delta} f(x/\delta),$$

where the scaling parameter δ is small. The scaled version of a blob is often used to get rid of any singularities which cause the function to blow up. For any value $\delta > 0$, the following holds:

$$\int_{-\infty}^{\infty} f_\delta(x) dx = \int_{-\infty}^{\infty} \frac{1}{\delta} f\left(\frac{x}{\delta}\right) dx = \int_{-\infty}^{\infty} f(z) dz = 1$$

where $z = x/\delta$ and at the same time $f_\delta(0) = f(0)/\delta$. From this, we see that for small values of δ , $f_\delta(0)$ is large, meaning that the peak of the blob is higher, while the blob is very narrow. On the other hand, if δ is large, the peak of the blob is lower, while the blob has a wider appearance.

Blobs, also known as cutoff functions, play an important role in one of the particle methods tested in this paper. Cutoff functions in 2D are of the form $f_\delta(\mathbf{x}) = \delta^{-2}f(|\mathbf{x}|/\delta)$, where $f \in C^2(\mathbb{R}^2)$ is a radially symmetric function. [2] defines f_σ to be a cutoff function of order $d + 2$ if f satisfies the following conditions:

- (C1) $\int f(|\mathbf{x}|)d\mathbf{x} = 1$,
- (C2) $\int \mathbf{x}^\beta f(|\mathbf{x}|)d\mathbf{x} = 0$ for $1 \leq |\beta| \leq d + 1$, and
- (C3) $\int |\mathbf{x}|^{d+2}|f(|\mathbf{x}|)d\mathbf{x} < \infty$

One characteristic of a cutoff function is that it is a good approximation to the Dirac delta function for small values of δ .

In our calculations, we will be using the following cutoff functions:

- The 4th order cutoff function

$$f(r) = \frac{1}{12\pi}[16e^{-r^2} - e^{-r^2/4}]$$

- The 6th order cutoff function

$$f(r) = \frac{1}{2\pi}(6 - 6r^2 + r^4)e^{-r^2}$$

Recall that a cutoff function of order $d+2$ means that all moments up until the $d+1$ moment is equal to zero, which is what is declared in condition (C2).

2.2 Diffusion Kernels

All the particle methods discussed require the presence of a diffusion kernel, denoted Λ_σ . $\Lambda(r)$ is a smooth, radially symmetric function that satisfies the following conditions for $d \geq 2$:

- (K1) $\int \mathbf{x}_i^2 \Lambda(|\mathbf{x}|)d\mathbf{x} = 2$ for $i = 1, 2$,
- (K2) $\int \mathbf{x}^\beta \Lambda(|\mathbf{x}|)d\mathbf{x} = 0$ for $3 \leq |\beta| \leq d + 1$,
- (K3) $\int |\mathbf{x}|^{d+2}|\Lambda(|\mathbf{x}|)d\mathbf{x} < \infty$, and
- (K4) $\widehat{\Lambda}(\mathbf{s}) \leq \widehat{\Lambda}(0)$

We also define the Fourier transform utilized in (K4) to be, for $g \in L^2(\mathbb{R}^2)$,

$$\widehat{g}(\mathbf{s}) = \int_{\mathbb{R}^2} g(\mathbf{x})e^{-is \cdot \mathbf{x}}d\mathbf{x}$$

(K1) through (K3) ensure that the error in the approximation of the Laplacian by the operator Q discussed later is $O(\sigma^d)$. A function Λ that satisfies (K1)-(K3) will be referred to as a kernel of order d .

While different than blobs, the diffusion kernels do retain certain characteristics that make them behave in a similar manner. One of these similarities deals with the

parameters h , the interparticle distance, and the numerical parameter σ . When we are using a blob (or kernel) to approximate a function, what we are doing is overlapping narrow blobs over the domain of the function. Two adjacent blobs must overlap to some extent in order to produce a smooth function approximation. If we have $\delta < h$, the blobs produced will be too narrow and will not sufficiently overlap to the extent needed to produce a good approximation. Instead, the approximation function will appear as an oscillating curve.

In our calculations, we will be using the following diffusion kernels:

- Second order:

$$\Lambda_1(r) = \frac{4}{\pi\sigma_1^2}e^{-q_1^2}, \quad q_1 = \frac{r}{\sigma_1}$$

- Fourth order:

$$\Lambda_2(r) = \frac{4}{\pi\sigma_2^2}[3 - q_2^2]e^{-q_2^2}, \quad q_2 = \frac{r}{\sigma_2}$$

where σ is the scaling parameter as in the case of the blobs. In order to make comparisons between Λ_1 and Λ_2 later in the paper, the parameters σ_1 and σ_2 must satisfy the condition $3\sigma_1^4 = \sigma_2^4$ to make $\Lambda_1(0) = \Lambda_2(0)$.

2.3 Particle Methods

The numerical methods studied here are based on discretizations of an integro-differential equation that approximates (2) by replacing the Laplacian with an integral operator. The integro-differential equation is:

$$\frac{\partial\Gamma}{\partial t} + (\mathbf{u} \cdot \nabla)\Gamma = \nu Q\Gamma, \quad \nabla \cdot \mathbf{u} = 0, \quad (4)$$

$$\Gamma(\mathbf{x}, 0) = \Gamma_0(\mathbf{x}), \quad \mathbf{x} \in \mathbb{R}^2, \quad (5)$$

where the operator Q is defined by

$$Q\Gamma(\mathbf{x}) = \frac{1}{\sigma^2} \int_{\mathbb{R}^2} [\Gamma(\mathbf{y}) - \Gamma(\mathbf{x})]\Lambda_\sigma(\mathbf{y} - \mathbf{x})d\mathbf{y}, \quad (6)$$

with σ being a numerical parameter and $\Lambda_\sigma(\mathbf{x}) = \sigma^{-2}\Lambda(|\mathbf{x}|/\sigma)$. We can also rewrite this equation as:

$$\begin{aligned} Q\Gamma(\mathbf{x}) &= \frac{1}{\sigma^2} \left(\int \Gamma(\mathbf{y})\Lambda_\sigma(\mathbf{y} - \mathbf{x})d\mathbf{y} - \int \Gamma(\mathbf{x})\Lambda_\sigma(\mathbf{y} - \mathbf{x})d\mathbf{y} \right) \\ &= \frac{1}{\sigma^2} \left(\int \Gamma(\mathbf{y})\Lambda_\sigma(\mathbf{y} - \mathbf{x})d\mathbf{y} - \Gamma(\mathbf{x}) \int \Lambda_\sigma(\mathbf{y} - \mathbf{x})d\mathbf{y} \right) \\ &= \frac{1}{\sigma^2} \int \Gamma(\mathbf{y})\Lambda_\sigma(\mathbf{y} - \mathbf{x})d\mathbf{y} - \frac{\lambda}{\sigma^2}\Gamma(\mathbf{x}) \end{aligned} \quad (7)$$

where $\lambda = \int \Lambda(|\mathbf{y}|)d\mathbf{y}$ is a constant. Since we know that $\Gamma(\mathbf{x}) = \int \Gamma(\mathbf{y})\bar{\delta}(\mathbf{y} - \mathbf{x})d\mathbf{y}$ where $\bar{\delta}$ is a two-dimensional Dirac delta, then equation (7) becomes:

$$\begin{aligned}
Q\Gamma(\mathbf{x}) &= \frac{1}{\sigma^2} \int \Gamma(\mathbf{y}) \Lambda_\sigma(\mathbf{y} - \mathbf{x}) d\mathbf{y} - \frac{\lambda}{\sigma^2} \int \Gamma(\mathbf{y}) \bar{\delta}(\mathbf{y} - \mathbf{x}) d\mathbf{y} \\
&= \frac{1}{\sigma^2} \int \Gamma(\mathbf{y}) (\Lambda_\sigma(\mathbf{y} - \mathbf{x}) - \lambda \bar{\delta}(\mathbf{y} - \mathbf{x})) d\mathbf{y}
\end{aligned} \tag{8}$$

The three numerical methods used to discretize (4) depend upon variations of our view of the operator Q . These methods are based on the versions of the integral operator Q displayed in (6), (7) and (8), where the parameter h represents the distance between particles:

1. Method A (PSE Method):

$$Q^h\Gamma(\mathbf{x}) = \frac{h^2}{\sigma^2} \sum_{j=1}^N [\Gamma(\mathbf{x}^j) - \Gamma(\mathbf{x})] \Lambda_\sigma(\mathbf{x} - \mathbf{x}^j). \tag{9}$$

2. Method B:

$$Q^h\Gamma(\mathbf{x}) = \frac{h^2}{\sigma^2} \sum_{j=1}^N \Gamma(\mathbf{x}^j) \Lambda_\sigma(\mathbf{x} - \mathbf{x}^j) - \frac{\lambda}{\sigma^2} \Gamma(\mathbf{x}) \tag{10}$$

3. Method C:

$$Q^h\Gamma(\mathbf{x}) = \frac{h^2}{\sigma^2} \sum_{j=1}^N \Gamma(\mathbf{x}^j) [\Lambda_\sigma(\mathbf{x} - \mathbf{x}^j) - \lambda f_\delta(\mathbf{x} - \mathbf{x}^j)] \tag{11}$$

For the operator Q^h in method C, it is required that a cutoff function f_δ (which approximates $\bar{\delta}(\mathbf{x})$) be of order $d + 2$ in order to approximate the Laplacian to order d . That is to say, it is necessary to choose a kernel Λ of order d and a cutoff f_δ of order $d + 2$, where the numerical parameters σ and δ satisfy $\sigma = c\delta$ for some fixed positive constant c . For our analysis we will be using $c = 1$, which means $\sigma = \delta$, since this choice seems to yield the best approximation for method C.

2.4 Conservation

Since we will be focusing on the case of heat diffusion for the study cases, then it becomes necessary to consider the laws of conservation that must be followed. That is to say that the total amount of heat has to be conserved. The amount of heat can be represented as $v(t) = \int_{\mathbb{R}^2} \Gamma(\mathbf{x}) dx dy$, and having it constant would mean $\frac{d}{dt} \int_{\mathbb{R}^2} \Gamma(\mathbf{x}) dx dy = 0$.

This can be derived as follows. Let Ω be a disc centered at the origin with boundary D . Then:

$$\frac{d}{dt} \int_{\Omega} \Gamma(\mathbf{x}) dx dy = \int_{\Omega} \frac{D\Gamma}{Dt}(\mathbf{x}) dx dy$$

Then, we notice that the left side of equation (2) is equal to the material derivative in the previous equation ($\frac{\partial \Gamma}{\partial t} + (\mathbf{u} \cdot \nabla)\Gamma = \frac{D\Gamma}{Dt} = \nu \Delta \Gamma$). So, we get:

$$\int_{\Omega} \frac{D\Gamma}{Dt}(\mathbf{x}) dx dy = \nu \int_{\Omega} \Delta \Gamma(\mathbf{x}) dx dy \quad (12)$$

Then, by using Gauss Theorem, equation (12) becomes:

$$\nu \int_{\Omega} \Delta \Gamma(\mathbf{x}) dx dy = \nu \int_D \nabla \Gamma(\mathbf{x}) \cdot \mathbf{n} dx dy$$

where \mathbf{n} is a vector on the plane normal to the curve D. The right side of the equation is an expression for the total flux that comes out of the system, which is zero if we consider a bounding curve D to be big enough. This condition is necessary for our approximation methods to be correct. This means that the particles on the boundaries should not have a significant change of heat level, otherwise the system would not conserve heat as it should.

3 Methods of Error Analysis

The three methods for approximating the solution of the convection-diffusion equation can be compared by considering study cases for which we have exact solutions. These cases and their results will be discussed in the following section. Nevertheless, in order to determine which is the best method we also need to be able to compare the different errors obtained from each case. We will focus on the study of two significant errors: the error concerning conservation, and the relative error in the solution.

3.1 Conservation Analysis

As it was described before, our study cases will consider the diffusion of heat for which conservation is applied. It was also mentioned that the total amount of heat ($\int_{\mathbb{R}^2} \Gamma(\mathbf{x}, t) dx dy = v(t)$) on the system should stay constant throughout time. Numerically, this quantity can be calculated by finding the total volume enclosed under the particles as time changes. In other words the ratio between the total amount of heat and the initial amount of heat should be one.

$$\frac{v(t)}{v(0)} = 1$$

The error will be measured by looking at the changes of this ratio throughout time. Figure-1 is an example of the kind of plot that we obtained from the conservation analysis. This plot displays the change of the heat ratio, which is the ratio described above, for the time interval observed.

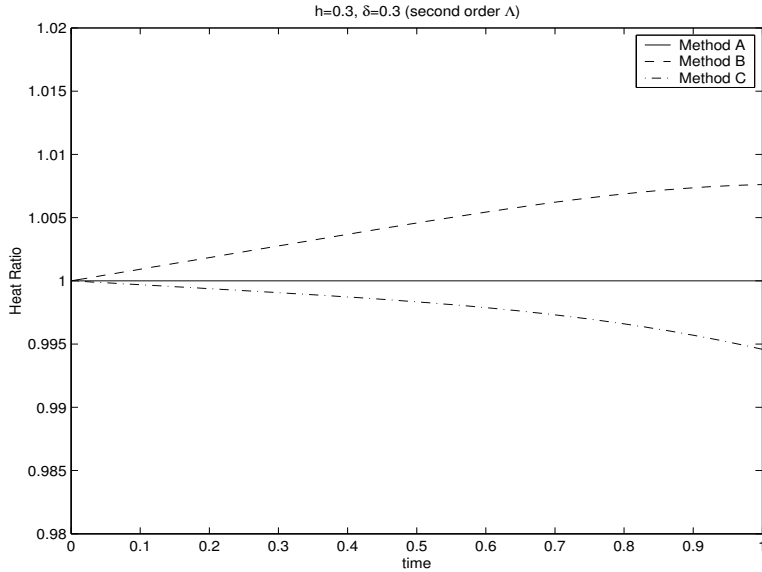


Figure 1: Heat Conservation Ratio

3.2 Relative Error

Our second method for error analysis deals with the relative error calculation. This error will be defined as the 2-norm of the difference between the exact and approximated solutions divided by the infinity norm of the exact solution. Symbolically, this is represented by:

$$\frac{\|\Gamma^h(\mathbf{x}, t) - \Gamma(\mathbf{x}, t)\|_2}{\|\Gamma(\mathbf{x}, t)\|_\infty} \quad (13)$$

The reason why we divide the difference by the infinity norm (which is the maximum of the function at the specific time) is to get an error that is not biased by the decreasing size of the function as time increases. The numerator in equation (13) is expected to decrease because the exact and approximated solutions approach zero as time increases. Therefore, a better way to observe the changes on the error is to divide this difference by the maximum of the function at the current time. Figure-2 shows a plot of the relative error. The axis labelled as "Error ratio" is the one representing the relative error.

4 Study Cases

In order to find the method that provides the most accurate approximation, we first need to define a problem whose solution is known so that we may have a reliable basis for our error analysis. Our best option is the case where the particles are motionless ($\mathbf{u} = \mathbf{0}$). By assuming this, the convection-diffusion equation simplifies to:

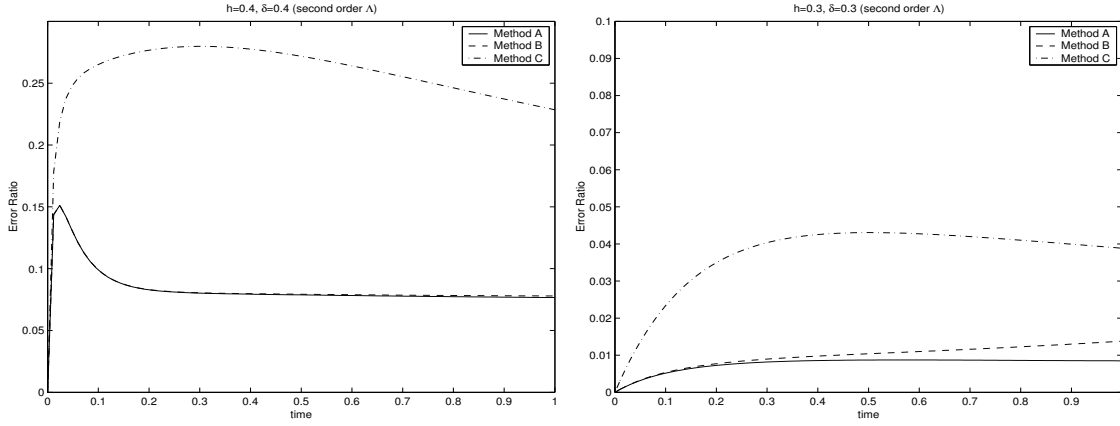


Figure 2: Relative Error

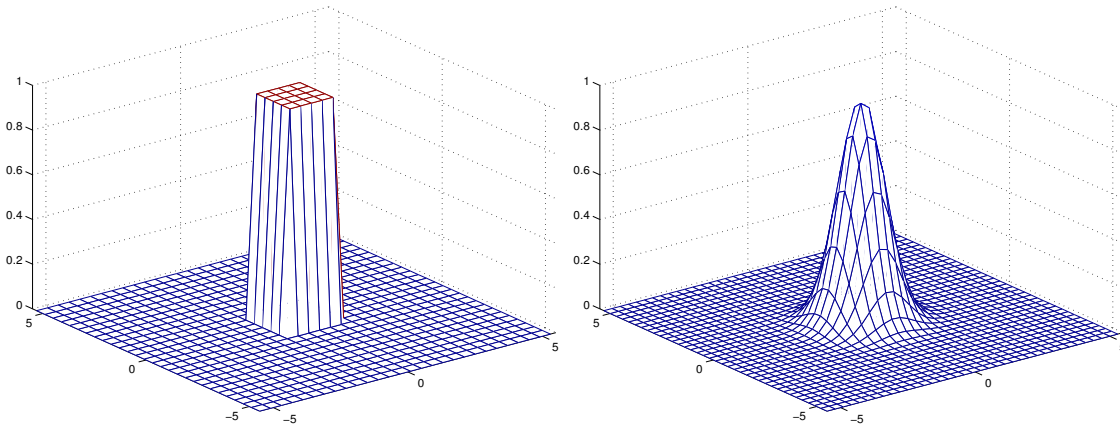


Figure 3: Initial Conditions ($t=0$)

$$\frac{\partial \Gamma}{\partial t} = \nu \left(\frac{\partial^2 \Gamma}{\partial x^2} + \frac{\partial^2 \Gamma}{\partial y^2} \right) = \nu(\Delta \Gamma) \quad (14)$$

where Γ would represent the temperature of the surface being modeled. We will be looking at two different cases which will compare the error results of a discontinuous initial condition with results of a continuous initial condition. The theoretical error bound discussed in the introduction only applies to initial conditions which have at least 4 continuous derivatives, the we are unable to place any bound on the error in the case where we are dealing with discontinuous initial conditions, which we investigate in Case 1. The analysis of this unknown error is discussed in the following section. In the case where our function is smooth, Case 2, we are able to utilize the theoretical error bound when we have a degree of 2 or 4, and we can hypothesize that the error plot will be parabolic in shape. The surface chosen for the error analysis in both cases is based on a finite surface. Figure-3 models the initial conditions for the two cases.

4.1 Case 1

We begin with the case where there is a discontinuity. The left side on figure-3 shows what the initial conditions look like for this case. We have a plate at a high temperature of 1 and all the other points at an initial heat level of zero. The exact solution to this problem, referred to as the fundamental solution for the diffusion equation in 2D in [1], is as follows:

$$\Gamma(\mathbf{x}, t) = \frac{1}{4\pi t} \int_{-1}^1 \int_{-1}^1 e^{-[(x-z_1)^2+(y-z_2)^2]/4t} dz_1 dz_2. \quad (15)$$

In computing the errors of our particle methods, Matlab (the program utilized in our research) aids us by providing the error function command, or Erf, where $\text{Erf}(x) = \frac{2}{\sqrt{\pi}} \int_0^x e^{-t^2} dt$. In order to take advantage of Matlab, we must manipulate our equation above in such a way that we may use the Erf command. The calculations necessary to make this transformation are as follows:

$$\begin{aligned} \Gamma(\mathbf{x}, t) &= \frac{1}{4\pi t} \int_{-1}^1 \int_{-1}^1 e^{-[(x-z_1)^2+(y-z_2)^2]/4t} dz_1 dz_2 \\ \Gamma(\mathbf{x}, t) &= \frac{1}{4\pi t} \int_{-1}^1 e^{-(x-z_1)^2/4t} dz_1 \int_{-1}^1 e^{-(y-z_2)^2/4t} dz_2 \end{aligned}$$

Using the change of variables method of solving integrals, we set $p = \frac{z_1-x}{2\sqrt{t}}$, making $dp = \frac{1}{2\sqrt{t}} dz_1$. Also, set $q = \frac{z_2-y}{2\sqrt{t}}$, making $dq = \frac{1}{2\sqrt{t}} dz_2$. Substituting these into our equation, we get

$$\begin{aligned} \Gamma(\mathbf{x}, t) &= \frac{1}{\pi} \int_{\frac{-1-x}{2\sqrt{t}}}^{\frac{1-x}{2\sqrt{t}}} e^{-p^2} dp \int_{\frac{-1-y}{2\sqrt{t}}}^{\frac{1-y}{2\sqrt{t}}} e^{-q^2} dq \\ \Gamma(\mathbf{x}, t) &= \frac{1}{\pi} \left(- \int_0^{\frac{-1-x}{2\sqrt{t}}} e^{-p^2} dp + \int_0^{\frac{1-x}{2\sqrt{t}}} e^{-p^2} dp \right) \left(- \int_0^{\frac{-1-y}{2\sqrt{t}}} e^{-q^2} dq + \int_0^{\frac{1-y}{2\sqrt{t}}} e^{-q^2} dq \right) \end{aligned}$$

In terms of the error function, we can write

$$\Gamma(\mathbf{x}, t) = \frac{1}{4} \left(-\text{Erf}f \left(\frac{-1-x}{2\sqrt{t}} \right) + \text{Erf}f \left(\frac{1-x}{2\sqrt{t}} \right) \right) \left(-\text{Erf}f \left(\frac{-1-y}{2\sqrt{t}} \right) + \text{Erf}f \left(\frac{1-y}{2\sqrt{t}} \right) \right) \quad (16)$$

We can now readily enter our solution into Matlab so that we may efficiently analyze our particle methods. This result was obtained for $\nu = 1$.

4.2 Case 2

For our second case, we define a continuous function that satisfies the diffusion equation. The left side of figure-3 shows the initial conditions for this case. This function is a decreasing exponential function and is defined as follows:

$$\Gamma(\mathbf{x}, t) = \frac{1}{1 + 4t} e^{-\left(\frac{ar^2}{1+4t}\right)} \quad (17)$$

where $r^2 = x^2 + y^2$.

In order to approximate the solution for this function, we will analyze the results obtained by considering the initial condition:

$$\Gamma(\mathbf{x}) = e^{-ar^2}, \quad a = 1$$

5 Results

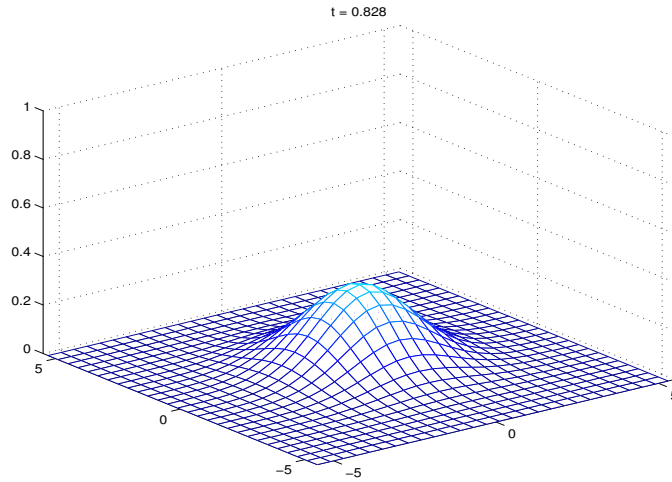


Figure 4: Heat Diffusion after $t=0$

Our simulations showed the diffusion of heat from the initial conditions displayed in figure-3. As time goes on, the heat diffuses similarly for both cases as displayed in figure-(4).

We ran simulations with $h = 0.4$, $\sigma = 0.4$, and δ values changing from 0.2 to 0.6. Remember that the δ value is the parameter for the cutoff function f_δ in method C, therefore these changes will only affect this method. Our observations show that the least relative error for method C comes from choosing $\sigma \approx \delta$. Based on these results we compared all these methods by using $\sigma = \delta$.

We also tried different values of σ for the first case by using h values between 0.2 and 0.6. For the cases of σ values smaller than h (see left side of figure-5) we noticed that the relative error curves behave oddly. This can be explained by some of the properties of the kernel function Γ that was defined. This function has some blob characteristics as discussed in the background section, which means that σ must be sufficiently large compared to h . If this is not the case, then the kernel approximation develops oscillations and large errors. For the cases when σ is greater than h (see

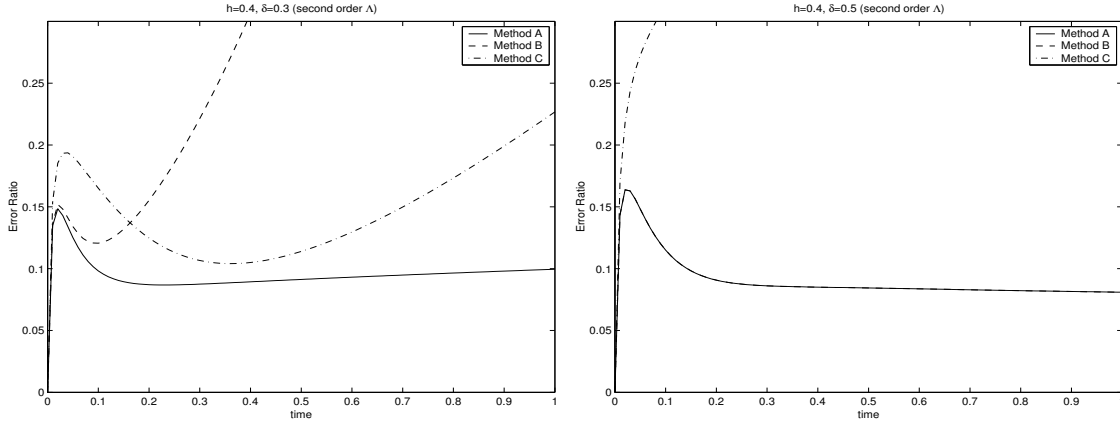


Figure 5: Relative Error ($h \neq \sigma$)

right side of figure-5), we noticed that the relative error for this case is higher than the error for $h = \sigma$ (see left side of figure-2).

In general, method A seems to be the best method for approximation. As we noticed from our data, method C is always the one that has the highest relative error. Method A and B appear to have almost identical error, but by zooming in enough we notice that method A in most cases has a lower error than B. We can also generalize and say that smaller values of h give better results, the values of h seem to affect the error in a degree higher than that of a linear function.

5.1 Comparing Cases

We now compare the results from our two study cases. Recall that the main difference between the cases is continuity of the initial conditions, where case 1 was discontinuous and case 2 was smooth and continuous. Our results show very similar results for the conservation analysis. These results will be discussed later in this paper. On the other hand the results for the relative error are very distinct. The error for the discontinuous case (as displayed on the left side of figure-2) shows how method A yields the best approximation and method C the worst. We also notice that these methods seem to have a peak at a time close to 0.05. The relative error plots for different values of h and σ for the first case look very similar to the one described before except for the scale. The peaks on the relative error plots seem to be caused by the discontinuity on the initial condition. This makes the error analysis complex and difficult to predict. For this reason, most of our analysis on the following section will be mostly based on results from case two. On the second case (as displayed on the right side of figure-2) we observed that the error plots start at zero and increase gradually to a more stable value. For this case we also observe that method A is the best approximation. As in the case before, we can see that the relative error plots for the different values of h are similar to the one described before, with the exception of the scale.

5.2 Relative Error Analysis for Case-2

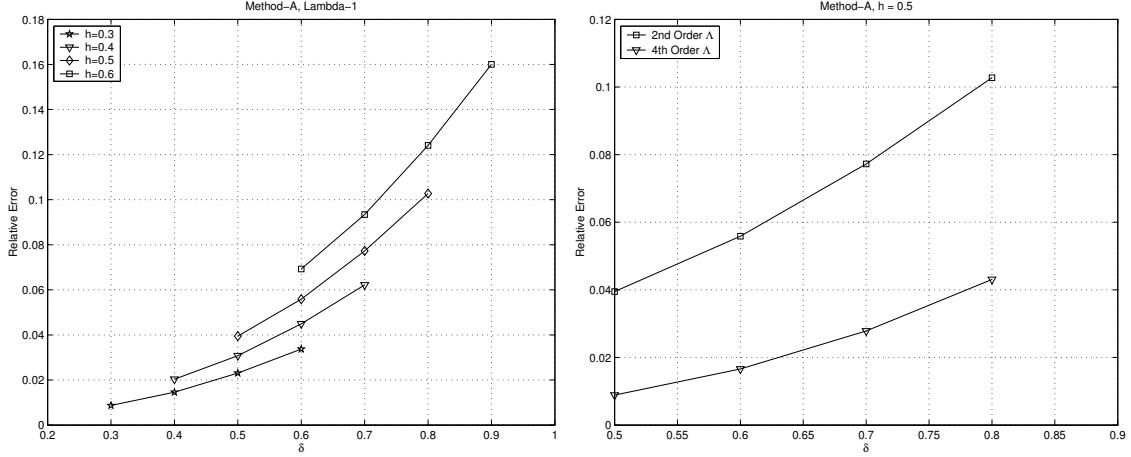


Figure 6: Relative Error for Method A

The general shape of the relative error plots was described earlier and can be observed on the left side of figure-2. These plots show how the error increases from 0 and seem to be bounded by a maximum. In general, method A seems to offer the best approximation for all the different values of h . On the other hand, method C seems to have some cases in which it blows up and has an error that seems to increase rapidly as shown in the error plots displayed in this paper.

Some of the data gathered for the analysis of how h and σ affect the relative errors is plotted on the left side of figure-6. In this plot we see the results for method A. Each curve displays how the error changes with respect to σ for specific values of h . The error curves shift up as the h increases. By the curvature of these lines, we speculate that they are of a degree higher than that of a linear function, which agrees with the theoretical error mentioned in the introduction. Equation (1) shows that the error is proportional to σ^d and other factors that combine σ and h . Our results show that σ^d is the predominant factor. Since we used a Λ of order two for this case, then the theory tell us that the error bound should be approximated to a square polynomial of σ .

The right plot on figure-6 shows a comparison between the second order and the fourth order Λ . For this comparison we chose $h = 0.5$ and $\sigma_1 = 0.5$ for the second order Λ . We also scaled the 4th order Λ to be comparable to the 2nd order Λ by choosing $\sigma_2 = 0.5(3)^{1/4}$. The choice of different Λ scales the error curve by a non-linear factor. To compare the degree between the second order Λ and the fourth order Λ , we divided the error values that we obtained. The results are displayed in Table-1.

When dividing the values from the fourth order by the values from the second order we notice that the ratio seems to be linearly related to h . To be more precise, the relation seems to be $\frac{\Lambda_2}{\Lambda_1} = \frac{h}{2}$. This is not a conclusive result since there is not enough data points to ensure it. However, this does show that the curve produced by

TABLE-1: Maximum Relative Error for Method A ($h = \sigma$)

h	Λ_1	Λ_2	$\frac{\Lambda_2}{\Lambda_1}$
0.5	0.0395	0.0089	0.2247
0.6	0.0559	0.0166	0.2971
0.7	0.0772	0.0279	0.3606
0.8	0.1028	0.0431	0.4191

the fourth order Λ is of a higher degree than the second order Λ , which is something expected from the theoretical bound of equation (1)

5.3 Conservation of Heat Analysis

When plotting the conservation of heat ratio, we notice that method A is also the one that approximates it the best. From the law of conservation of energy we know that heat should be conserved. Therefore, the volume under our simulation should stay the same. Our results (see figure-1) show that Method A always stays constant, while method B and C tend to increase or decrease depending on the values of σ and h .

Method A follows some laws of conservation that the other methods do not. If we consider the case of heat diffusion, we mentioned before that the total amount of heat has to be conserved. The amount of heat can be represented as in equation(12). The conservation section in the background gives some more details about how conservation should be satisfied.

From our results in the background section, we can conclude that the rate of change of the total amount of heat is equal to the integral of the Laplacian of Γ and can be approximated as: $\int_{\mathbb{R}^2} \Delta \Gamma dx dy \approx \sum_{k=1}^N (\Delta \Gamma_k) h^2$. And, we also know that the Laplacian of Γ is approximated by using equation (9) for method A. Combining these two results we obtain:

$$\begin{aligned} \int_{\mathbb{R}^2} \Delta \Gamma dx dy &\approx \sum_{k=1}^N \left(\frac{h^2}{\sigma^2} \sum_{j=1}^N [\Gamma_j - \Gamma_k] \Lambda(\vec{x}_k - \vec{x}_j) \right) h^2 \\ &= \frac{h^4}{\sigma^2} \left(\sum_{k=1}^N \sum_{j=1}^N \Gamma_j \Lambda(\vec{x}_k - \vec{x}_j) - \sum_{j=1}^N \sum_{k=1}^N \Gamma_k \Lambda(\vec{x}_j - \vec{x}_k) \right) = 0 \end{aligned}$$

The result is zero since both of these sums are equivalent. This stems from the fact that the only difference is in the indices. Considering this, we notice that method A is constructed to maintain the conservation of heat.

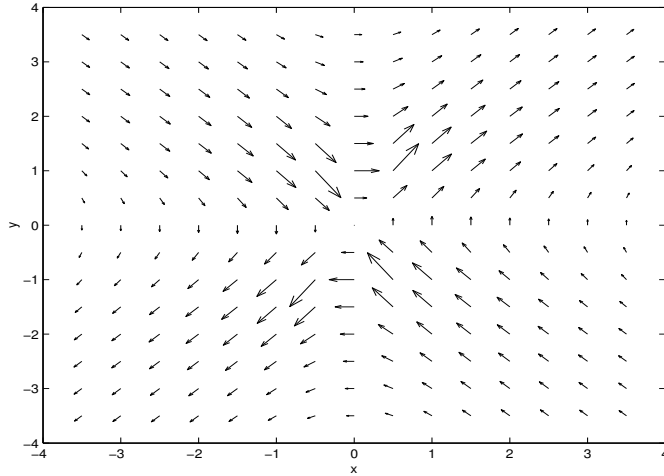


Figure 7: Stokeslet flow with 2 Forces

6 Modeling Diffusion Cases For Particular Flows

Using Method A, which we have determined to provide the best approximation of the solution to the convection diffusion equation, we now model the heat diffusion where the particles are moved by a particular flow. We have chosen to study the particular case of the Stokeslet flow. We define the two-dimensional Stokeslet as:

$$\vec{u}(\vec{x}) = -\vec{f}_0 \ln r + \frac{(\vec{f}_0 \cdot \vec{x})\vec{x}}{r^2}, \quad (18)$$

where $r^2 = x^2 + y^2$.

This flow is known to be incompressible, meaning that $\frac{\partial u_1}{\partial x} + \frac{\partial u_2}{\partial y} = 0$ for $r \neq 0$.

This is now ready to be entered into our program to run the simulation of the diffusion. We use a Λ of order four and $h = 0.4$, and $\sigma = 0.4(3)^{1/4}$ as discussed in the background section for scaling purposes.

The modeling of the particles is based on an equally spaced grid, which works very well when we are in a situation where there is no flow. However, once the particles start to move, there is going to be deformation, meaning that there may be clustering of particles in some areas, leaving areas of blank space. This deformation causes an increase in the error, making approximations that are not favorable. From previous research, it is known that there are ways to alleviate the consequences of the deformation. One such method is regridding, which consists of allowing the particles to move with respect to the flow until a certain time when deformation begins to take place. At this point, the simulation is stopped so that the grid can be redrawn and the particles repositioned by interpolating their current heat levels. By repeating this method as many times as necessary, we can reduce the error and make better approximations.

In our model, we have introduced two forces which are opposite in direction, but not along the same line (see figure-7). The opposing forces flow past one another

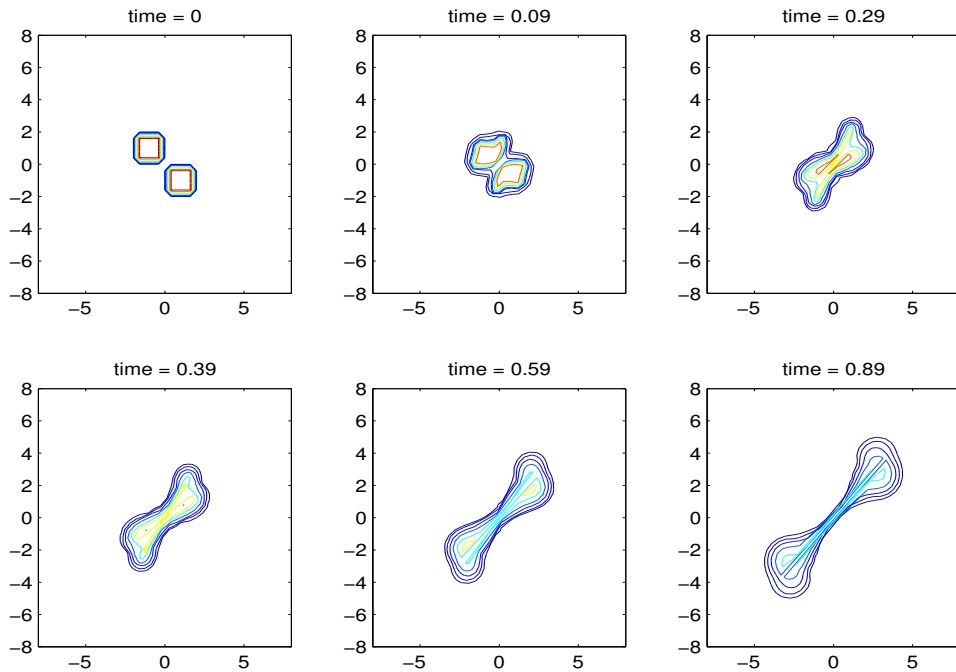


Figure 8: Stokeslet flow with 2 Forces

parallel, creating torque and movement that can be seen in the velocity field on figure-7. As the flow pushes the particles in diagonally towards the origin, the forces expel the particles away from the origin at the opposite slope from which they came. The contour plots (figure-8) shows a top view of the flow at certain times. We begin with two separate areas of heat, as shown in the upper left picture. After a short time, the forces applied causes a merging of the areas with a decrease in the amount of heat. As even more time elapses, the opposing force acts upon the area, causing deformation in a diagonal direction opposite from the first merge. For the remainder of the time, the movement of the heat continues in this manner, with more heat loss as time goes by. We are left with a figure that resembles an oar, with two large areas of heat located diagonally from each other with a thin bridge joining them. We must remember that this results are not completely accurate since a repositioning of the grid was not part of the calculations for this simulation. This means that the approximation does not converge to the solution as it was described before.

7 Conclusion

Our results and analysis show how method A appears to be the best method for numerically solving convection-diffusion equation. Our analysis of the two cases, the first discontinuous and the second continuous, show how the relative-error in all of the methods is dependent on h and σ . From our observations, we can conclude that this dependency is higher than that of the degree of a linear function, which seems

to agree with the theoretical error bound for the continuous case. For the analysis of conservation of heat we also noticed that method A has a built-in structure that makes it conserve the total amount of heat. However, this does not ensure the absence of error.

Finally, these methods of approximation can also be used for the cases where there is a prescribed flow. However, there are many other conditions that must be considered for these cases. We have to consider the deformation of the original grid on the flow, and do a repositioning of the points in order to obtain good results.

Acknowledgements

We would like to thank Dr. Ricardo Cortez for his patience and his guidance in this research project. We would also like to thank Alexander Villacorta and Angela Gallegos for their help and support throughout our work. Much gratitude to Dr. Herbert Medina and Dr. Ivelisse Rubio for giving us the opportunity to participate in SIMU, a program that has helped us mature intellectually and emotionally. To our fellow SIMU students, thank you for sharing all the moments of joy as well as the moments of tears. This work was funded by the National Science Foundation (NSF), grant no. DMS-9987901, and the National Security Agency (NSA), grant no. MDA-904-02-1-006.

References

- [1] L.C. Evans, *Partial Differential Equations*, American Mathematical Society, Rhode Island, 1998.
- [2] R. Cortez, *Covergence of High-Order Deterministic Particle Methods for the Convection-Diffusion Equation*, Communications on Pure and Applied Mathematics: Volume L, John Wiley and Sons, Inc. NY. (1997), 1235-1260.
- [3] C. Pozrikidis, *Introduction to Theoretical and Computational Fluid Dynamics*, Oxford University Press, (1997), New York.